

# RAKOMO: Reachability-Aware K-Order Markov Path Optimization for Quadrupedal Loco-Manipulation

Mattia Risiglione<sup>1,\*</sup>, Abdelrahman Abdalla<sup>1,\*</sup>, Victor Barasuol<sup>1</sup>,  
 Kim Tien Ly<sup>2</sup>, Ioannis Havoutis<sup>2</sup> and Claudio Semini<sup>1</sup>

**Abstract**—Legged manipulators, such as quadrupeds equipped with robotic arms, require motion planning techniques that account for their complex kinematic constraints in order to perform manipulation tasks both safely and effectively. However, trajectory optimization methods often face challenges due to the hybrid dynamics introduced by contact discontinuities, and tend to neglect leg limitations during planning for computational reasons. In this work, we propose *RAKOMO*, a path optimization technique that integrates the strengths of K-Order Markov Optimization (KOMO) with a kinematically-aware criterion based on the *reachable region* defined as *reachability margin*. We leverage a neural-network to predict the margin and optimize it by incorporating it in the standard KOMO formulation. This approach enables rapid convergence of gradient-based motion planning – commonly tailored for continuous systems – while adapting it effectively to legged manipulators, successfully executing loco-manipulation tasks. We benchmark RAKOMO against a baseline KOMO approach through a set of simulations for pick-and-place tasks with the HyQReal quadruped robot equipped with a Kinova Gen3 robotic arm.

## I. INTRODUCTION

Mobile manipulators are increasingly used in everyday activities due to their ability to perform tasks in industrial, domestic, and natural environments. Successful operations in the real world require the robot to reach and manipulate objects while avoiding collisions with both their own structure and the surrounding environment. The enhanced mobility provided by legs has motivated the robotics community to explore legged systems as mobile bases for manipulators. For these multi-limbed systems, referred to as legged manipulators, it is crucial to plan whole-body motions that are aware of the leg limitations, in order to avoid compromising the robot’s balance and performance in terms of tracking. Motion planning specifically addresses this problem by providing a set of collision-free configurations that respect the robot’s limitations.

In the literature, two powerful techniques for robot motion planning have been proposed: sampling-based and optimization-based planning, the latter often referred to as trajectory optimization (TO). Sampling-based methods, such as Rapidly Exploring Random Trees (RRT) and Probabilistic Roadmaps (PRM) [1], can theoretically converge to an optimal solution if one exists, but tend to suffer from a slow convergence time. By contrast, optimization-based planning generally yields smoother trajectories that are compatible

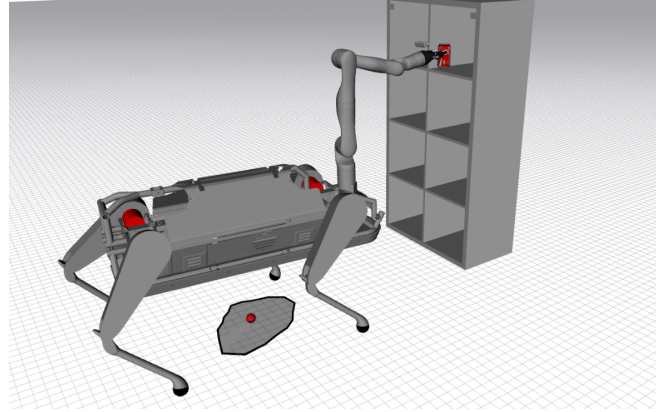


Fig. 1: Simulation screenshot of IIT’s HyQReal with a Kinova Gen3 robotic arm placing a can on a shelf using a reachability-aware KOMO.

with real-time requirements. Despite the risk of converging to locally optimal or unfeasible robot poses, we adopt TO in this work given that its convergence time is essential for the advancement of long-term planning [2], [3]. Recently, the robotics community has shown significant interest in using TO to solve task-and-motion planning (TAMP) problems, where for each task evaluated, a motion planning problem is computed to test kinematic and/or dynamic feasibility [4]. In the general formulation of TO, an objective function prioritizing path length, time, smoothness, and energy consumption is minimized under running and boundary constraints. Motion planning techniques such as CHOMP [5], STOMP [6], TrajOpt [7] and KOMO [8] discretize the problem and explore or approximate gradient information to drive the initial guess to the optimum. Their success has been proven for autonomous drone flight, underwater vehicle missions [9], and pick-and-place tasks with mobile robots (e.g. a PR2 robot [5]).

Trajectory optimization becomes more challenging for legged systems due to their inherently complex dynamical model, driven by nonlinear dynamics, strong coupling among actuated legs and the unactuated base, and the high dimensionality of the overall configuration space. Additionally, complexity scales up when the robot’s motion has to be optimized for additional limbs that are involved in non-locomotive tasks. Some prior approaches [10], [11] address such complexity by simplifying the system to a six degrees-of-freedom (DOF) base, planning the entire whole-body

<sup>1</sup>Dynamic Legged Systems Lab, Istituto Italiano di Tecnologia (IIT), Genova, Italy, {name.surname}@iit.it.

<sup>2</sup>Oxford Robotics Institute, University of Oxford, UK.

\*Equal contribution.

kinematic motions with this simplified representation, neglecting the effect of the legs.

The use of reduced-order models [10], [11] neglects the leg joint limitations during planning. Different approaches attempt to embed such information in the model without explicitly considering contact forces nor joint limits. A simple approach constrains the position of the base relative to the feet through box constraints [12]. These constraints result in conservative approximation of the kinematic limits and provide no metric for optimizing kinematic feasibility. On the other hand, authors in [13] introduce kinematic feasibility by learning the probability density of the CoM positions with respect to the feet locations. Alternatively, researchers also defined 2D regions where if a reference point, e.g., center of mass (CoM) position, lies inside then: *a*) friction constraints on the contact forces and motor's actuation limits are respected, namely the *feasible region* [14]; *b*) the joint-position limits are respected and leg singularities are avoided, namely the *reachable region* [15]. A more recent work [16] proposes a function approximator to estimate the so-called *feasibility margin*, defined as the shortest-distance between the instantaneous capture point (ICP) and the feasible region's boundary. Additionally, the authors in [16] proposed the margin optimization within a TO formulation to ensure dynamic locomotion robustness.

### A. Contributions

In this work, we propose an efficient trajectory optimization method for legged loco-manipulation that combines the efficiency of reduced modeling and feasibility of joint-level constraints. Explicitly modeling each leg joint introduces  $n_c n_j N$  joint decision variables, where  $n_c$  is the number of contacts,  $n_j$  is the number of joints in each leg, and  $N$  is the planning horizon. This choice significantly increases the problem complexity and computational time. To mitigate this, as proposed in [10], [11] we employ a simplified model of the legged robot (such as shown in Fig. 2) at a cost of neglecting any leg joint-level constraint. To address this limitation, we introduce an efficient representation of the joint-kinematic constraints using the *reachability margin* – a metric defining the shortest distance from the horizontal projection of the base position to the boundaries of the reachable region. Inspired by [16], we utilize a Multi-Layer Perceptron (MLP) to learn the *reachability margin*. We decide to incorporate the network into a KOMO formulation to prevent the robot's base from reaching heights and orientations that would push its legs beyond their reachability limits. This can occur for a legged manipulator whenever the end-effector has to reach very high or very low targets, as we show in the results section. An alternative approach could have been to impose empirical limits on the robot's base height and orientations. However, this method risks setting overly conservative constraints. By employing a KOMO formulation, we gain numerical advantages due to the emergence of a banded cost/constraints Jacobian and a banded-symmetric Hessian, as described in [17]. These properties make Gauss-Newton solvers well-suited to solve such problems. The complexity of KOMO is linear on the

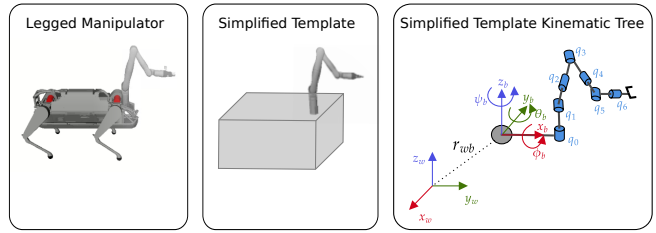


Fig. 2: Overview of the template model used by KOMO for planning. On the left, the full model of the robot is shown. In the center, the simplified template consists of a box with a robotic arm attached to it. On the right is the kinematic tree constructed for KOMO using the simplified template.

number of waypoints and polynomial on the dimension of the robot configuration space [8]. Despite its advantages, KOMO has been applied so far to fixed-based manipulators and omnidirectional wheeled robots [2], [18].

At each iteration, the KOMO's trajectory is passed to an inverse-dynamics whole-body (IDWB) controller that solves a one shot Quadratic Programming problem for generating the robot actuation commands. In summary, with the goal of extending gradient-based planning tailored for non-holonomic mobile manipulators to legged manipulators and successfully execute these plans online, we highlight the main contribution as:

- We introduce an efficient trajectory planning method for legged manipulators that leverages simplified robot models while effectively incorporating joint-kinematic constraints without resorting to full kinematic representation of the legs. This reduces the number of decision variables by  $n_c n_j N$ , resulting only in minimal computational overhead to simplified methods.
- We propose a loco-manipulation planning strategy suitable for all legged commercial robots that operate with a black-box locomotion controller, where direct control of individual legs is not available to the control designer [11][19]. Instead, the robot can only be steered through velocity inputs. The proposed strategy allows to create whole-body motions that inherently account for the kinematic limitations of the legs without explicitly modeling or incorporating them into the planning process, enabling more effective planning motion generation even in the absence of low-level leg control.

The paper is organized as follows: Sec. II and Sec. III presents, respectively, the motion planning and control of the robot. Section IV presents the proposed simulations and discusses the results. Section V concludes the paper.

## II. MOTION PLANNING

In this section, we introduce the *reachability margin* and formulate the reachability-aware formulation of KOMO, named as *RAKOMO*.

### A. Reachability Margin

In order for the planner to provide kinematically feasible trajectories when using a simplified template as in Fig. 2, it is crucial to consider the influence of the leg joint limits

on the base motion. However, determining the resulting kinematic limits of the robot base states (e.g. roll, pitch, and height) is highly challenging because they cannot be treated as independent from each other. Additionally, such base kinematic limits are strongly dependent on the relative distance between the base and each foot. Such a relationship, instead, can be described in an efficient manner using the *reachable region* introduced in [20]. The *reachable region* describes the set of all base positions the robot can achieve for the given contact position and base orientation, where the joint constraints would be respected. Similar to the approach of [16], we utilize the *reachable region* in an optimization problem by defining a metric of reachability. This metric helps to guide the optimization of the base's motion to enhance kinematic feasibility and ensure efficient use of the robot's reachable workspace.

The reachability metric, defined as *reachability margin*, is the distance between the current base position and the closest boundary of the reachable region. The computation of the *reachability margin* is achieved through the following steps:

- 1) computation of the *reachable region*; and 2) computation of the minimum distance between the horizontal projection of the base position and the edges of the *reachable region*.

The *reachable region* can be obtained by mapping the kinematic constraints of the robot (defined in joint space) to the task-space (the Cartesian space where the base is defined). A ray-casting search is done to find the furthest point in the Cartesian space where the joint limits are still respected, i.e., the vertices of the region. As a result from the nature of the leg kinematic chain, the *reachable region* is, in general, a non-convex set.

Given that the feasible region is non-convex, we resort to computing the *reachability margin* by iteratively computing the margins to all the edges of the region (obtained from the vertices) and find the minimum value. The minimum distance between the base and each edge  $i$  of the region can be computed using

$$d_i = \frac{|a_{iw}x_{wb} + b_{iw}y_{wb} + c_i|}{\sqrt{a_i^2 + b_i^2}} \quad (1)$$

where  $wx_{wb}$  and  $wy_{wb}$  are the x and y coordinates of the base w.r.t the world frame, respectively, and  $a_i$ ,  $b_i$ , and  $c_i$  are real constants of the line equation of the edge, with  $a_i$  and  $b_i$  being both non-zero. Introducing  $d = [d_1, \dots, d_{N_e}]$ , where  $N_e$  is the number of edges of the region, a *reachability margin*  $m$  is obtained using  $m = \min(d)$ .

To incorporate the *reachability margin* in a gradient-based optimization problem, we need to be able to compute its gradient w.r.t. its inputs. Given the non-differentiable nature of the iterative algorithm used to obtain the region, this can only be achievable through the finite-difference of the numerical computation. This is considerably inefficient as the computation of one region can take, on average, 30 to 40 ms (with the gradient computation requiring over 1 sec). Instead, we proceed to approximate the *reachability margin* through training an MLP network.

Note that given it is needed to generate trajectories for the robot's base (see Section II-B), we have defined the

*reachability margin* in (1) using the robot's base position. However, in reality, the *reachable region* is only affected by the configuration of the feet relative to the base. Therefore, to simplify the training of the network, the input to the *reachable region* and the MLP can be defined as  $\mathbf{x}_r = [{}_b\mathbf{e}_z, {}_b\mathbf{x}_{bf_i}, \dots, {}_b\mathbf{x}_{bf_{Nc}}]$  where  ${}_b\mathbf{e}_z$  is the unit vector representing the z-axis of the world frame in the robot base frame,  ${}_b\mathbf{x}_{bf_i}$  is the i-th foot position relative to the base frame (and expressed in the base frame), and  $N_c$  is the number of feet in contact with the ground. Additionally, to optimize the margin with respect to the base position, we can use the relationship

$${}_b\mathbf{x}_{bf_i} = {}_b\mathbf{R}_w(\mathbf{x}_{bf_i} - \mathbf{x}_{wb}) \quad (2)$$

where  ${}_b\mathbf{x}_{bf_i}$  is the i-th foot position relative to the base frame (and expressed in the world frame) and  $\mathbf{x}_{wb}$  denotes the base Cartesian position (expressed in the world frame). Finally, the network output is the scalar value of the *reachability margin*  $m$ .

The architecture of the network is composed of 3 hidden layers, where the first layer has 512 neurons, the second layer has 256 neurons, and the third layer has 128 neurons. The activation function used in the hidden layers is the ReLU function, while the output layer has no activation function. The dataset is generated by sampling the input variables from uniform distributions centered around nominal operating values. The network is trained on a dataset composed of  $5 \cdot 10^6$  samples, which was verified to be sufficient to reach a plateau in the prediction performance. Given that we can warm start the TO within the operating conditions and that the system is physically constrained to the kinematic boundaries, generalization outside the selected range is not needed. The time taken to compute the inference and the gradient of the network is on average 10 ms and 100 ms, respectively. This allows for the margin to be utilized efficiently in TO.

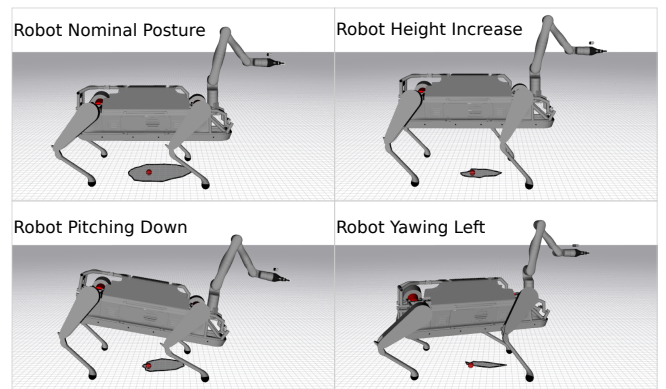


Fig. 3: Illustration of the reachable region (grey area on the ground) for HyQReal in different postures: on the top-left, the robot in a nominal posture; top-right, when the robot height is increased; bottom-left, when the robot pitches down; and bottom-right, when the robot yaws to the left. The red sphere inside the region represents the projection of the robot's base position.

## B. K-Order Markov Path Optimization - KOMO

KOMO is an efficient method for solving motion planning problems introduced by Marc Toussaint in 2014 [21]. It represents a path as a sequence of waypoints, each defined as a kinematic robot configuration. A robot configuration can be seen as a set of joints connected by rigid links. We parameterize the robot configuration space as  $\mathbf{q} = [{}_{\mathbf{w}}\mathbf{x}_{wb}, {}_{\mathbf{w}}\mathbf{q}_b, \mathbf{q}_a] \in \mathbb{R}^{6+n_a}$  where  ${}_{\mathbf{w}}\mathbf{q}_b$  denotes the base orientation expressed in the world frame using Euler angles, and  $q_1, \dots, q_{n_a}$  correspond to the manipulator's joint angles with  $n_a$  the number of joints. The goal is to find a trajectory as a set of robot-configuration  $\mathbf{q}_0, \dots, \mathbf{q}_N$  that minimizes

$$\begin{aligned} \min_{\mathbf{q}_{0:N}} \quad & \mathbf{f}(\mathbf{q}_{0:N}) \\ \text{s.t.} \quad & \mathbf{g}(\mathbf{q}_{0:N}) \leq 0, \\ & \mathbf{h}(\mathbf{q}_{0:N}) = 0 \end{aligned} \quad (3)$$

where  $\mathbf{f} \in \mathbb{R}$  is the cost functional, and  $\mathbf{g} \in \mathbb{R}^{n_g}$  and  $\mathbf{h} \in \mathbb{R}^{n_h}$  are inequalities and equality constraints, respectively.

The inherent  $k$ -order Markovian property means that a robot configuration at time  $t$ , defined by  $\mathbf{q}_t$ , is influenced by a history of previous robot configuration up to the  $k$ -th order, i.e.  $\mathbf{q}_{t-k:t}$ . This property is useful to create costs or constraints only dependent on a group of  $k$ -tuples states, and break older temporal dependencies. Hence, we can rewrite (3) as

$$\begin{aligned} \min_{\mathbf{q}_{0:N}} \quad & \sum_{t=0}^N \mathbf{f}_t(\mathbf{q}_{t-k:t})^T \mathbf{f}_t(\mathbf{q}_{t-k:t}) \\ \text{s.t.} \quad & \forall t : \mathbf{g}_t(\mathbf{q}_{t-k:t}) \leq 0, \\ & \mathbf{h}_t(\mathbf{q}_{t-k:t}) = 0 \end{aligned} \quad (4)$$

with  $\mathbf{f}_t \in \mathbb{R}$ ,  $\mathbf{g}_t \in \mathbb{R}^{n_{g_t}}$  and  $\mathbf{h}_t \in \mathbb{R}^{n_{h_t}}$ . Not all cost and constraint functions have the same order  $k$ ; it depends on the derivative order of the kinematic quantity involved. Specifically, for penalizing positions, velocities, and accelerations, we need respectively  $k$  being of order 0, 1, and 2.

### Objective

The final trajectory should be smooth and penalize overall joint displacement from the starting robot joint configuration. Hence, we introduce here two type of costs:

$$\mathbf{f}_t = \|\mathbf{q}_t - \mathbf{q}_0\|^2 \quad (5)$$

$$\mathbf{f}_t = \|\mathbf{q}_t - 2\mathbf{q}_{t-1} + \mathbf{q}_{t-2}\|^2 \quad (6)$$

Additionally, we want to optimize the reachability margin  $m$  around a desired value  $\epsilon^*$  along the robot's trajectory

$$\mathbf{f}_t = \|\epsilon^* - m(\mathbf{q}_t)\|^2 \quad (7)$$

where  $m$  is a function of the base position and orientation (through  ${}_b\mathbf{R}_w$ ) as shown in (2).

### Equality Constraints

Considering an object to grasp at a certain position (or a target position to place an object) defined as  $\mathbf{z} \in \mathbb{R}^3$ , we

define the kinematic constraint to reach such desired end-effector's target position as

$$\mathbf{h}_t = \mathcal{H}(\mathbf{q}_t) - \mathbf{z} \quad (8)$$

being  $\mathcal{H}(\mathbf{q}_t)$  the differentiable kinematic model of the legged manipulator. We adopt a robot-centric perspective, preferring to express costs for the arm's end-effector which can lead to desired object motion poses. Hence, we can avoid to increase the dimensionality of the solution space, by not including rigid objects poses in  $\mathbf{q}$  during the different time slices. Handling objects implies including them into the robot's kinematic tree, once each contact with the object is established.

### Inequality Constraints

To avoid self-collisions and environmental-collisions in the final trajectory we impose the following constraints:

$$\mathbf{g}_t = -d(\mathcal{K}_i(\mathbf{q}_t), \mathcal{K}_j(\mathbf{q}_t)) - (r_i + r_j) \leq 0 \quad i \neq j \quad (9)$$

$$\mathbf{g}_t = -d(\mathcal{K}_i(\mathbf{q}_t), \mathcal{K}_j(\mathbf{x}_o)) - (r_i + r_o) \leq 0 \quad \forall i \in \mathcal{S}_r \quad (10)$$

with  $\forall i, j \in \mathcal{S}_r$ ,  $\forall o \in \mathcal{S}_o$  and  $d$  being the Euclidean distance between two collision primitives  $\mathcal{K}$  with sphere-radius  $r$  each. The two sets  $\mathcal{S}_r$  and  $\mathcal{S}_o$  denote, respectively, the subsets of robot and object meshes. Additionally, to respect arm joint limits and leg joint limits (through the reachability margin) we include

$$\mathbf{g}_t = \begin{cases} \mathbf{q}_{a_t} - \bar{\mathbf{q}}_a \leq 0 \\ \underline{\mathbf{q}}_a - \mathbf{q}_{a_t} \leq 0 \end{cases} \quad (11)$$

$$\mathbf{g}_t = \epsilon - m(\mathbf{q}_t) \leq 0 \quad (12)$$

with  $\underline{\mathbf{q}}_a$  and  $\bar{\mathbf{q}}_a$  being the lower and upper bound for the arm joint limits, and  $\epsilon \in \mathbb{R}^{\geq 0}$  a small safety margin threshold.

### Solver

The formulation of the optimal problem (4) is general enough for any non-linear programming solver, given differentiable functions  $\mathbf{f}_t$ ,  $\mathbf{g}_t$  and  $\mathbf{h}_t$ . The MLP problem in (4) is solved with Augmented Lagrangian via Newton's method adopting line search. The Markovian property leads to having banded Jacobian of the costs/constraints (obtained by partial derivative with respect to  $\mathbf{q}$ ) because first-order dependencies are local ( $\mathbf{q}_t$  depends only on  $k$  previous configurations and not all the past states). The non-zero entries of the cost/constraint Jacobian associated to (7) and (12) are expressed for the rotational coordinates of the base as

$$\frac{\partial m}{\partial q_b} = (\nabla m_g)^T \frac{\partial \mathbf{g}}{\partial q_b} \quad \forall q_b \in {}_w\mathbf{q}_b \text{ we} \quad (13)$$

where  $(\nabla m_g)$  is the gradient of the neural network output with respect to the vector  $\mathbf{g}$ . The Jacobian related to the translational coordinates can be obtained as

$$\frac{\partial m}{\partial x_{wb}} = (\nabla m_{b\mathbf{x}_{bf}})^T \frac{\partial_b \mathbf{x}_{bf}}{\partial x_{wb}} \quad \forall x_{wb} \in {}_w\mathbf{x}_{wb} \quad (14)$$

where  $(\nabla m_{b\mathbf{x}_{bf}})$  is the gradient of the neural network output with respect to feet positions resulting in  $\frac{\partial_b \mathbf{x}_{bf}}{\partial x_{wb}} = -{}_b\mathbf{R}_w$  from (2).

## Collision Avoidance

In this work, we rely on the Flexible-Collision library (FCL) [22] to perform collision and penetration queries. In particular, we leverage the computation of depth penetration between two convex polytopes using the Expanding Polytope Algorithm (EPA) [23], and we use the Gilbert-Johnson-Keerthi (GJK) algorithm [24] to compute the Euclidian distance between the queried convex shapes used in (10).

## III. MOTION CONTROL

The motion planner outputs a set of robot joint configurations,  $\mathbf{q}$ , containing the base and arm degrees of freedom. According to the robot state, linear interpolation is performed between the current state and the next desired waypoint from KOMO. The number of waypoints for each dimension of the vector  $\mathbf{q}$  is determined as  $N = \max(\frac{\Delta q_i}{v_i^{\max}} f_s) \forall i = 1, \dots, 6 + n_a$ , with  $\Delta q_i$  being the displacement between two consecutive configurations along the  $i$ -th dimension,  $f_s$  being the control frequency, and  $v_i^{\max}$  being the maximum velocity of the  $i$ -th direction. The desired waypoint, denoted by  $\mathbf{q}^*$  (containing the base and the arm desired position states), is provided to the dynamic whole-body controller (WBC) [25], with the exception that the desired joint accelerations, denoted by  $\ddot{\mathbf{q}}^d$ , are computed as

$$\ddot{\mathbf{q}}^d = \mathbf{K}_p(\mathbf{q}^* - \mathbf{q}) + \mathbf{K}_d(\dot{\mathbf{q}}^* - \dot{\mathbf{q}}) + \mathbf{K}_i \int_0^t (\mathbf{q}^* - \mathbf{q}) \quad (15)$$

with  $\mathbf{K}_p$ ,  $\mathbf{K}_d$ , and  $\mathbf{K}_i$  being respectively the proportional, derivative, and integral gain matrices.  $\mathbf{q}$  and  $\dot{\mathbf{q}}$  represent, respectively, the current joint position and velocity, while  $\mathbf{q}^*$  and  $\dot{\mathbf{q}}^*$  represent, respectively, the desired joint position and velocity.

To control the robot torso, a desired wrench  $\mathbf{W}_b^d$  (to be rendered by the WBC) is defined w.r.t. the quadruped's base:

$$\mathbf{F}_b^d = \mathbf{K}_b(\mathbf{x}_b^d - \mathbf{x}_b) + \mathbf{D}_b(\dot{\mathbf{x}}_b^d - \dot{\mathbf{x}}_b) \quad (16)$$

$$\mathbf{T}_b^d = \mathbf{D}_r(\mathbf{w}_b^d - \mathbf{w}_b) + \mathbf{K}_r \mathbf{e}_r \quad (17)$$

where  $\mathbf{F}_b^d$  and  $\mathbf{T}_b^d$  are respectively the desired force and moment on the base, i.e.  $\mathbf{W}_b^d = [\mathbf{F}_b^{dT}, \mathbf{T}_b^{dT}]^T$ . We define  $\mathbf{e}_r$  as the base rotational error,  $\mathbf{D}_r \in \mathbb{R}^{3 \times 3}$  the diagonal derivative gain matrix, and  $\mathbf{K}_r \in \mathbb{R}^{3 \times 3}$  the diagonal proportional gain matrix. The WBC solves for the stacked vector of generalized accelerations  $\dot{\mathbf{u}} = [\ddot{\mathbf{q}}_b^T, \ddot{\mathbf{q}}_l^T, \ddot{\mathbf{q}}_a^T]^T \in \mathbb{R}^{6+n_l+n_a}$ , which is composed of the linear and angular accelerations of the base  $\ddot{\mathbf{q}}_b = [\ddot{\mathbf{x}}_b^T, \ddot{\mathbf{w}}_b^T]^T \in \mathbb{R}^6$  and the rest of the leg  $\ddot{\mathbf{q}}_l^T$  and arm  $\ddot{\mathbf{q}}_a^T$  joint accelerations. The WBC optimization problem solves for the vector of decision variables  $\xi = [\dot{\mathbf{u}}^T, \mathbf{F}_g^T]^T$ , from which, using the robot's inverse dynamics, yields desired torques  $\boldsymbol{\tau} = [\boldsymbol{\tau}_l^T, \boldsymbol{\tau}_a^T]^T$  computed as:

$$\begin{bmatrix} \boldsymbol{\tau}_l \\ \boldsymbol{\tau}_a \end{bmatrix} = \begin{bmatrix} \mathbf{M}_{lb} & \mathbf{M}_l & \mathbf{M}_{la} \\ \mathbf{M}_{ab} & \mathbf{M}_{al} & \mathbf{M}_a \end{bmatrix} \begin{bmatrix} \ddot{\mathbf{q}}_b \\ \ddot{\mathbf{q}}_l \\ \ddot{\mathbf{q}}_a \end{bmatrix} + \begin{bmatrix} \mathbf{h}_l \\ \mathbf{h}_a \end{bmatrix} - \begin{bmatrix} \mathbf{J}_{st,l}^T \\ \mathbf{J}_{st,a}^T \end{bmatrix} \mathbf{F}_g - \begin{bmatrix} \mathbf{0}_{l \times 3n_c} \\ \mathbf{J}_{c,a}^T \end{bmatrix} \mathbf{F}_e \quad (18)$$

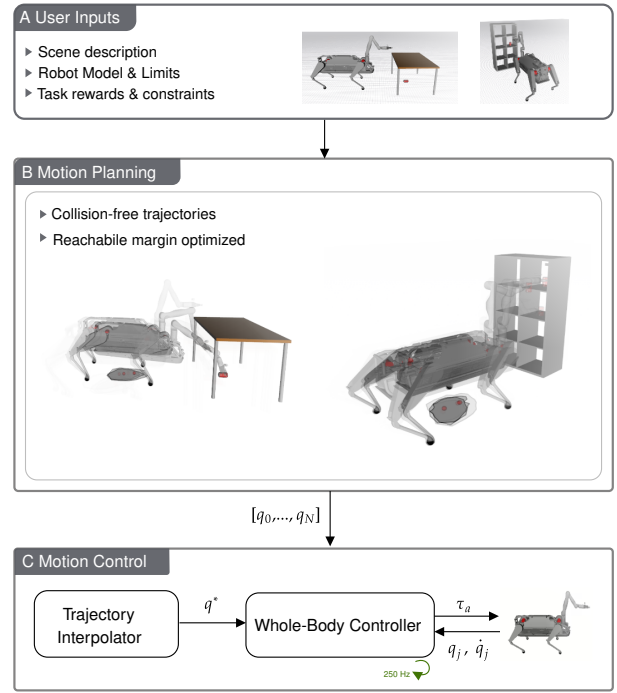


Fig. 4: Overview of the control architecture for the planning and execution of loco-manipulation tasks. (A) User inputs and task scenario definition. (B) The motion generation part via KOMO calculates collision-free trajectories, taking into account the maximization of the reachable region margin. (C) The trajectories, or desired robot configurations, are interpolated and tracked with a dynamic whole-body controller running at 250 Hz.

where  $\mathbf{F}_g \in \mathbb{R}^{3n_c}$  is the robot's foot ground reaction forces, with  $n_c$  being the number of contact feet, and  $\mathbf{F}_e \in \mathbb{R}^3$  denotes the external force acting on the arm's end-effector.  $\mathbf{F}_g$  and  $\mathbf{F}_e$  are mapped respectively to the base through the contact Jacobians  $\mathbf{J}_{st}^T$  and  $\mathbf{J}_e^T$ .  $\mathbf{J}_{e,a}^T \in \mathbb{R}^{6 \times n_a}$  is the Jacobian matrix from base to end-effector.

## IV. RESULTS

We conducted a set of simulations to validate the proposed approach using our legged manipulator, HyQReal with a Kinova Robotic Gen3 arm. The simulations were performed using Gazebo as a physics simulator. Throughout this work we leverage KOMO's solver [26] to solve full path optimization problems for a fixed number of body configurations  $N$  equal to 15. For collision avoidance, we modeled the quadruped's trunk as a bounding box and provided sphere-swept convex meshes around each link of the robotic arm. In all simulations, we considered the robot in a stance configuration, i.e. with all four feet on the ground and  $\mathbf{x}_{bf_i}$  fixed. The integration of dynamic gait and contact sequence optimization is left for future work. We designed two simulation scenarios to assess the results of the *baseline* approach (KOMO without the inclusion of the reachable regions) and our proposed approach *RAKOMO*: 1) grasping an object from a low height; and 2) picking and placing an object on high shelves. All the simulations discussed in this

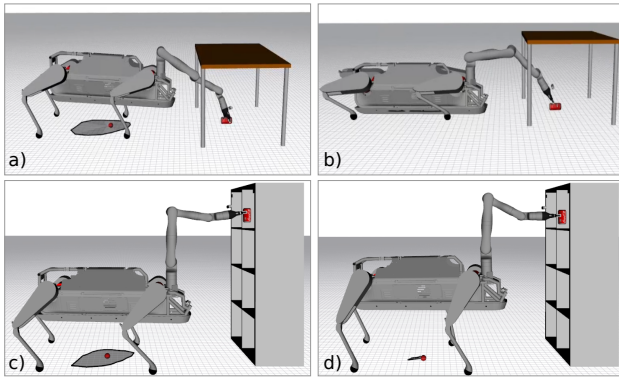


Fig. 5: Simulation scenarios: grasping low-height object using a) RAKOMO and b) baseline planner; and picking and placing an object on high shelves using c) RAKOMO and d) baseline planner.

section are also included in the accompanying video.

#### A. Grasping low-height object

In the first simulation, the robot is required to grasp a bottle underneath a table. The scenario is depicted in Fig. 5a,b. For the whole task duration, the penalization weight for the arm's position deviations in the cost function (5) was set to be 10 times lower than the weight for penalizing base positions. This choice allows to exploit the arm's reachability as much as possible before the optimizer finds body postures in support of the arm. The desired value for the *reachability margin*  $\epsilon^*$  in (7) is set to  $0.15m$  and the minimum feasibility margin  $\underline{\epsilon}$  is set to  $0.05m$ .

Results showed that introducing the *reachability margin* regularization in (7) helps the optimizer to find body poses with better leg kinematic margins along the robot's trajectory. When using the *baseline* approach, the robot is unaware of the leg limitations. As a consequence, the quadruped's trunk lowers excessively, leading to unfavourable leg configurations. This results in a mismatch in the final end-effector position. As shown in Fig. 6, the reachability margin starts increasing around  $5s$  because the robot's nominal height starts decreasing, bringing the left-front (LF) Hip-Flexion Extension (HFE) joint towards the center of its kinematic range. However, the same joint retracts more as the base height decreases, resulting in the margin dropping considerably until the motion is stopped when the robot belly hits/touches the ground. On the other hand, RAKOMO manages to keep the same joint, i.e. LF HFE closer towards the middle of the workspace throughout the grasping task, resulting in a margin centered around the optimal value  $\epsilon^*$ .

The possibility of deploying the algorithm on quadruped robots, for online replanning, is maintained in both cases: the time to compute a solution according to the KOMO stopping criteria is  $104ms$  for the baseline and  $270ms$  for RAKOMO. Although this represents an increase of approximately 2.6 times, RAKOMO remains significantly more efficient compared to running KOMO on the full robot model, which would be composed of four additional kinematic chains (legs) leading to 12 additional joints (see Fig. 2). Given that the computational complexity scales cubically with the

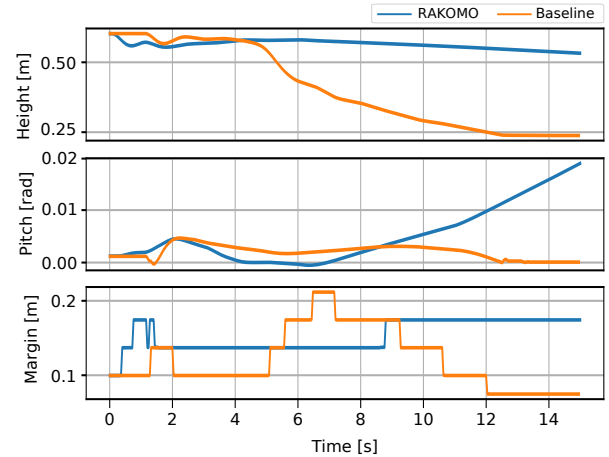


Fig. 6: Comparison of the *reachability margin* for the executed low-height object grasping motion planned using RAKOMO and the baseline approach. RAKOMO (blue) achieves a higher minimum value than the baseline approach (orange).

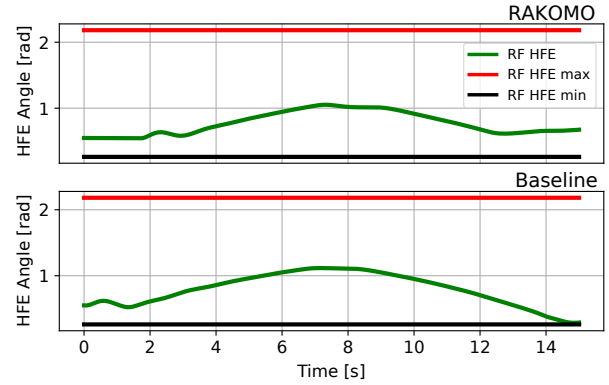


Fig. 7: Evolution of the HFE joint of the right front leg during the execution of the high-shelf object manipulation motion. The red and black horizontal lines represent the maximum and minimum joint limits, respectively. The optimization of the *reachability margin* in RAKOMO results in the joint angle lying closer to the center of the joint range of motion (Top). Meanwhile, the baseline approach shows the joint angle getting close to the joint limit (Bottom).

number of joints [27], these extra kinematic chains would lead to an estimated computation time increase of 7 times for the same setup, what would make an online implementation difficult.

#### B. Pick and place of object on a high shelf

In the second simulation scenario, the robot is positioned in front of a bookcase and tasked with moving a soda can from a lower shelf to an upper one. The scenario is depicted in Fig. 5c,d. To ensure accurate grasping and placement, we added two 0-order constraints as shown in (8) to enforce the object's grasping at the initial time and the place position at the final time. Both RAKOMO and the baseline approach KOMO explore the planar DOF of the base to help the arm reach the object and move away from the shelf before placing the item on the upper shelf. However, during the final phase

of the task, the baseline approach proceeds to raise the base to an excessive height (as shown in Fig. 5d) due to the lack of awareness of the leg kinematic limits. As a result, the right-front leg (RF) HFE joint reaches its lower bound limit towards the end of the task, as illustrated in Fig. 7. In contrast, with RAKOMO, the robot's base height and orientation are maintained closer to more *reachable* values, ensuring better alignment with the robot's kinematic limits. The difference in terms of body posture around the end of the task is shown in Fig. 5c. From a computational perspective, the time to compute a solution according to the KOMO stopping criteria for the solver is 120ms, and for RAKOMO it is 285ms.

## V. CONCLUSIONS

In this work, we presented a novel methodology for motion planning in legged manipulators that integrates a reachability margin within the K-Order Markov Optimization (KOMO) framework. By leveraging supervised learning to model the reachability margin (i.e. the shortest distance from the base's horizontal projection to the boundary of the leg's reachable region), we incorporated leg kinematic limitations directly into the motion planning process without explicitly modeling all the leg joints. This approach allows for efficient planning on a reduced-order model while ensuring that the generated motions do not push the robot's legs beyond their kinematic limits. We presented simulation results involving IIT's 140kg HyQReal quadruped equipped with a Kinova Gen3 manipulator, performing tasks such as grasping low-height objects and picking and placing items on high shelves. The results demonstrated that our method successfully generates whole-body motions that respect leg limitations. As a future direction, we aim to extend the approach for walking scenarios. Additionally, we aim at considering also dynamic limitations of the robot, such as torque limits.

## REFERENCES

- [1] S. Karaman and E. Frazzoli, "Sampling-based algorithms for optimal motion planning," *The International Journal of Robotics Research*, vol. 30, no. 7, pp. 846–894, 2011. [Online]. Available: <https://doi.org/10.1177/0278364911406761>
- [2] K. T. Ly, V. Semenov, M. Risiglione, W. Merkt, and I. Havoutis, "R-lgp: A reachability-guided logic-geometric programming framework for optimal task and motion planning on mobile manipulators," in *2024 IEEE International Conference on Robotics and Automation (ICRA)*, 2024, pp. 14917–14923.
- [3] J.-P. Sleiman, F. Farshidian, and M. Hutter, "Versatile multicontact planning and control for legged loco-manipulation," *Science Robotics*, vol. 8, no. 81, p. eadg5014, 2023. [Online]. Available: <https://www.science.org/doi/abs/10.1126/scirobotics.adg5014>
- [4] M. Toussaint, "Logic-geometric programming: An optimization-based approach to combined task and motion planning," in *Proceedings of the 24th International Conference on Artificial Intelligence*, ser. IJCAI'15. AAAI Press, 2015, p. 19301936.
- [5] N. Ratliff, M. Zucker, J. A. Bagnell, and S. Srinivasa, "Chomp: gradient optimization techniques for efficient motion planning," in *Proceedings of the 2009 IEEE International Conference on Robotics and Automation*, ser. ICRA'09. IEEE Press, 2009, p. 40304035.
- [6] M. Kalakrishnan, S. Chitta, E. Theodorou, P. Pastor, and S. Schaal, "Stomp: Stochastic trajectory optimization for motion planning," in *2011 IEEE International Conference on Robotics and Automation*, 2011, pp. 4569–4574.
- [7] J. Schulman, Y. Duan, J. Ho, A. X. Lee, I. Awwal, H. Bradlow, J. Pan, S. Patil, K. Goldberg, and P. Abbeel, "Motion planning with sequential convex optimization and convex collision checking," *The International Journal of Robotics Research*, vol. 33, pp. 1251 – 1270, 2014. [Online]. Available: <https://api.semanticscholar.org/CorpusID:893094>
- [8] M. Toussaint, "Komo: Newton methods for k-order markov constrained motion problems," in *arXiv preprint arXiv:1407.0414*, 2014.
- [9] M. Xanthidis, N. Karapetyan, H. Damron, S. Rahman, J. Johnson, A. O'Connell, J. M. OKane, and I. Rekleitis, "Navigation in the presence of obstacles for an agile autonomous underwater vehicle," in *2020 IEEE International Conference on Robotics and Automation (ICRA)*, 2020, pp. 892–899.
- [10] S. Zimmermann, M. Busenhart, S. Huber, R. Poranne, and S. Coros, "Differentiable collision avoidance using collision primitives," *2022 IEEE/RSJ International Conference on Intelligent Robots and Systems (IROS)*, pp. 8086–8093, 2022. [Online]. Available: <https://api.semanticscholar.org/CorpusID:248266394>
- [11] S. Zimmermann, R. Poranne, and S. Coros, "Go fetch! - dynamic grasps using boston dynamics spot with external robotic arm," in *2021 IEEE Int. Conf. on Robotics and Automation*, 2021, pp. 4488–4494.
- [12] P. Fankhauser, M. Bjelonic, C. Dario Bellicos, T. Miki, and M. Hutter, "Robust rough-terrain locomotion with a quadrupedal robot," in *2018 IEEE Int. Conf. on Robotics and Automation*, 2018, pp. 5761–5768.
- [13] J. Carpentier, R. Budhiraja, and N. Mansard, "Learning Feasibility Constraints for Multi-contact Locomotion of Legged Robots," in *Robotics: Science and Systems*, vol. Proceedings of Robotics Science and Systems, Cambridge, MA, United States, July 2017, p. 9p. [Online]. Available: <https://faas.hal.science/hal-01526200>
- [14] R. Orsolino, M. Focchi, S. Caron, G. Raiola, V. Barasuol, D. G. Caldwell, and C. Semini, "Feasible region: An actuation-aware extension of the support region," *IEEE Transactions on Robotics*, vol. 36, no. 4, pp. 1239–1255, 2020.
- [15] A. Abdalla, M. Focchi, R. Orsolino, and C. Semini, "An efficient paradigm for feasibility guarantees in legged locomotion," *IEEE Transactions on Robotics*, vol. 39, no. 5, pp. 3499–3515, 2023.
- [16] R. Orsolino, S. Gangapurwala, O. Melon, M. Geisert, I. Havoutis, and M. Fallon, "Rapid stability margin estimation for contact-rich locomotion," in *2021 IEEE/RSJ International Conference on Intelligent Robots and Systems (IROS)*, 2021, pp. 8485–8492.
- [17] M. Toussaint, "A tutorial on newton methods for constrained trajectory optimization and relations to slam, gaussian process smoothing, optimal control, and probabilistic inference," in *Geometric and Numerical Foundations of Movements*, 2017. [Online]. Available: <https://api.semanticscholar.org/CorpusID:43673663>
- [18] J. Kamat, J. Ortiz-Haro, M. Toussaint, F. T. Pokorny, and A. Orthey, "Bitkomo: Combining sampling and optimization for fast convergence in optimal motion planning," in *2022 IEEE/RSJ International Conference on Intelligent Robots and Systems (IROS)*, 2022, pp. 4492–4497.
- [19] I. Taouil, G. Turrisi, D. Schleich, V. Barasuol, C. Semini, and S. Behnke, "Quadrupedal footstep planning using learned motion models of a black-box controller," *2023 IEEE/RSJ Int. Conference on Intelligent Robots and Systems (IROS)*, pp. 800–806, 2023. [Online]. Available: <https://api.semanticscholar.org/CorpusID:260125842>
- [20] A. Abdelrahman, M. Focchi, R. Orsolino, and C. Semini, "The reachable region: a fast kinematic feasibility criterion for legged locomotion," in *I-RIM Conference*, 2020.
- [21] M. Toussaint, "Newton methods for k-order markov constrained motion problems," 2014.
- [22] J. Pan, S. Chitta, and D. Manocha, "Fcl: A general purpose library for collision and proximity queries," in *2012 IEEE International Conference on Robotics and Automation*, 2012, pp. 3859–3866.
- [23] G. Van Den Bergen, "Proximity queries and penetration depth computation on 3d game objects," in *Game developers conference*, vol. 170, 2001, p. 209.
- [24] J. P. Linahan, *A Geometric Interpretation of the Boolean Gilbert-Johnson-Keerthi Algorithm*. Villanova University, 2015.
- [25] M. Risiglione, V. Barasuol, D. G. Caldwell, and C. Semini, "A whole-body controller based on a simplified template for rendering impedances in quadruped manipulators," in *2022 IEEE/RSJ International Conference on Intelligent Robots and Systems (IROS)*, 2022, pp. 9620–9627.
- [26] M. Toussaint, "Komo tutorial," 2023. [Online]. Available: <https://marctoussaint.github.io/robotics-course/>
- [27] T. Marc, "A tutorial on newton methods for constrained trajectory optimization and relations to slam, gaussian process smoothing, optimal control, and probabilistic inference," *Geometric and Numerical Foundations of Movements*, 2017. [Online]. Available: <https://doi.org/10.1007/978-3-319-51547-2-15>